SAND99-2410J

RECEIVED
OCT 20 1999
OSTI

A Comparison of Kretschmann-Raether Angular Regimes for Measuring Changes in Bulk Refractive Index

K. J. Kasunic

Sandia National Laboratories

Albuquerque, NM 87185

June 1, 1999

Abstract

We compare 2 angular regimes for the measurement of changes in the real refractive index of bulk fluid analytes. The measurements are based on the use of the Kretschmann-Raether configuration to sense a change in reflectivity with index. Specifically, we numerically simulate the relative sensitivities of the total internal reflection (TIR) and surface-plasmon resonance (SPR) regimes. For a fixed-angle apparatus, the method which gives the greatest change in reflectivity varies with metal film thickness. For films thicker than the skin depth, the SPR regime is the most sensitive to index changes. For thinner films, however, the TIR angle is then dominant, with increases in sensitivity on the order of 75% for 10 nm gold or silver media.

DISCLAIMER

This report was prepared as an account of work sponsored by an agency of the United States Government. Neither the United States Government nor any agency thereof, nor any of their employees, make any warranty, express or implied, or assumes any legal liability or responsibility for the accuracy, completeness, or usefulness of any information, apparatus, product, or process disclosed, or represents that its use would not infringe privately owned rights. Reference herein to any specific commercial product, process, or service by trade name, trademark, manufacturer, or otherwise does not necessarily constitute or imply its endorsement, recommendation, or favoring by the United States Government or any agency thereof. The views and opinions of authors expressed herein do not necessarily state or reflect those of the United States Government or any agency thereof.

DISCLAIMER

Portions of this document may be illegible in electronic image products. Images are produced from the best available original document.

1 Introduction

Two angular regimes for the measurement of changes in the real refractive index of fluid analytes may be classified as total internal reflective (TIR) and surface-plasmon resonant (SPR). Perhaps the most common method is the TIR, found in many optical laboratories in the form of the Abbe refractometer [1]. This instrument utilizes the total internal reflection which occurs at a high-to-low dielectric interface (prism-to-analyte, e. g.), creating evanescent waves along the interface for a range of incident angles which depend on the ratio of indices. When referenced against a known prism index, the TIR technique can measure analyte index to an absolute accuracy of 1 part in 10^5. This accuracy is a result of experimental parameters such as prism flatness and angular resolution, rather than fundamental limitations [2].

These same evanescent waves, when propagating along a metal-dielectric interface, can excite free-electron resonances called surface plasmons. This effect has been used in a number of device applications, typically as optical chemical sensors to measure changes in analyte contaminant concentration associated with changes in index [3]-[11]. Experimentally, SPR effects are observed as a sharp mimimum in reflectivity as the angle of incidence is varied; as shown below, changes in the analyte index shift this minimum. Monitoring the resulting change in reflectivity at a fixed angle can then be used to measure the change in analyte. As with TIR, variations in refractive index to 1 part in 10^5 have been measured with this technique [5].

Our experiments, however, require the use of an electrode to electrically excite the analyte. Our design is also intended to measure index changes in a compact, portable device with the sensitivity of the Abbe refractometer. We are thus led to the Kretschmann-Raether configuration for plasmon excitation [10] shown in Fig. 1. The experimental apparatus for measuring index changes with SPR are then numerous [10]. The simplest approach is to measure the angular shift in reflectivity as the analyte is varied. For the case of SPR, the important feature to be monitored is the reflectivity minimum. The sensitivity is limited, however, because information contained in the slope of the

reflectivity curve is ignored. A more useful approach, then, is to select a fixed measurement angle, and obtain the *change* in reflectivity as index variations shift the reflectivity-versus-angle curve [4]-[6], [10]. In this way, both the slope and the shift of the reflectivity curve are utilized.

The goal of this paper is to evaluate the relative sensitivities of the TIR and SPR regimes using the fixed-angle Kretschmann-Raether apparatus. We make no attempt to predict the limits on analyte index change that can be measured for each regime. Rather, we assume an index change and numerically simulate the change in reflectivity using the methods of Mansuripur [12]. Note that our results do not consider specific experimental parameters such as laser linewidth, manufacturing tolerances, temperature and dispersion compensation, etc. Also note that our calculations do not apply to the typical case of an adsorptive metal surface, to which a thin film of target species may adhere. Rather, we are concerned with measuring changes in bulk refractive index, for which we assume a controlled analyte environment.

2 Theory

In this section, we briefly review the theory governing each of the 2 regimes. We start with the TIR method. As mentioned above, this common technique is the principle governing the Abbe refractometer, which can measure refractive indices to approximately 1 part in 10^5. Since our emphasis is on measuring changes in index as a measure of analyte contamination, we approach this method from a slightly different point of view. Specifically, to compare the sensitivity of TIR with SPR, we look at how the TIR (or critical) angle changes with analyte index. In the absence of a metal film, this angle is given by the familiar equation

$$\theta_{TIR} = sin^{-1}(n_a/n_p) \tag{1}$$

where n_a and n_p are the (real) indices of the analyte and prism, as shown in Fig. 1. An immediate disadvantage of this method is that the index of the prism must be larger than that of the analyte. A

typical example of how the reflectivity varies with internal prism angle θ_p for a transverse-magnetic (TM, or p-polarized) field is shown in Fig. 2.

The rationale for the Kretschmann-Raether SPR geometry is a phase-matching of the incident field with free electron (plasma) excitations at the metal-analyte surface. These surface plasmons have a wavenumber k_{sp} given by [7]

$$k_{sp} = \frac{\omega}{c}\mathrm{Re}\left[\frac{1}{\epsilon_a} + \frac{1}{\epsilon_m(\omega)}\right]^{-1/2} \tag{2}$$

where ω is the frequency of the incident field, c is the speed of light in vacuum, ϵ_a $(=n_a^2)$ is the dielectric constant of the analyte, and $\epsilon_m(\omega)$ is the complex dielectric constant of the metal. For phase matching to occur, k_{sp} must equal k_x, the x-component of the wavenumber of the incident light in the prism

$$k_x = \omega n_p \sin\theta_p / c \tag{3}$$

Note that Eqs. (2)-(3) are readily solved for the angle at which a reflection minimum occurs, known as the surface-plasmon angle θ_{sp}. This angle is seen to depend on n_a, thus providing the basis for the SPR technique.

For free electrons at long wavelengths away from the bulk plasma frequency ω_p, the frequency dependence of $\epsilon_m(\omega)$ is given by [10]

$$\epsilon_m(\omega) = 1 - \frac{\omega_p^2}{\omega^2} \tag{4}$$

Substituting this result in Eq. (2), we obtain a plasmon dispersion equation for $\omega(k_{sp})$, with a frequency which asymptotically approaches $\omega_p/(1+\epsilon_a)^{1/2}$ for large k_{sp}. Graphically, the phase matching needed for surface plasmons is found from the intersection of this asymptotic curve with the straight line given by Eq. (3). This cannot occur unless the slope of Eq. (3) is less than that of the asymptotic curve at the origin (see, for example, Ref. [7], Fig. 3), easily shown to be c/n_a. This compares with a slope of $c/n_p sin\theta_p$ for the prism dispersion. The 2 slopes are equal when

$sin\theta_p = n_a/n_p$, which is identical to the TIR condition given by Eq. (1). Surface plasmons can therefore only be generated by evanescent waves. Also note the importance of the prism index; the SPR technique thus suffers from the same disadvantage as the TIR.

3 Numerical Results and Discussion

In this section, we present numerical results comparing the sensitivity of each of the 2 regimes to changes in analyte index. Our modeling is based on Diffract [12], a commercially-available physical-optics software package. TIR results are shown in Fig. 2, where we plot the TM-reflectivity R_{TM} as a function of internal prism angle θ_p. The figure assumes a prism index n_p=1.457 for fused silica at λ=0.633 μm, and bulk analyte indices n_a =1.330 and 1.334. Neglecting Fresnel losses at the entrance to the prism, the results show the well-known approach to a reflectivity of unity as θ_p approaches the TIR condition $\theta_{TIR} \approx 65.9$ degrees given by Eq. (1). Both the slope of this curve near the TIR angle and the shift with index indicates the change in reflectivity ΔR_{TM}. This is quantified in Fig. 3, where we plot the angular dependence of ΔR_{TM} for the given Δn_a=0.004. The figure clearly illustrates the greatest sensitivity to index changes near the critical angle.

For the SPR regime, we take 10 nm as a practical lower limit on film thickness [13]. Fig. 4 then shows how R_{TM} for the Kretschmann-Raether arrangement varies with θ_p for gold films of thickness t=10, 20, and 50 nm. For clarity, we plot the curves for only 1 index (n_a=1.330). The significant features of this curve are twofold. As discussed above, SPR requires an evanescent angle $\theta_{sp} > \theta_{TIR}$. Up to a point, these effects are enhanced for the thicker metallic films, with 50 nm giving approximately optimum response for gold. However, the thicker films also reduce the sensitivity of the TIR effect, as the reflectivity is large for angles less than θ_{TIR} for a film thickness approaching the skin depth δ of the metal ($\approx$ 32 nm for the assumed complex index N_g= 0.13+i3.16 [14] for gold). This is illustrated in Fig. 5, where we plot ΔR_{TM} for Δn_a=0.004. The results clearly show the greater sensitivity to analyte changes near the TIR angle for the 10 nm

film; alternatively, the SPR regime dominates for the 50 nm film. Comparing the 2 sensitivities for the assumed prism, electrode, and analyte indices, we see that the critical angle has approximately 75% greater sensitivity than the SPR angle for a 10 nm gold film. Additional simulations show that a detection scheme with a sensitivity of 1% is required for measuring a bulk index change Δn_a=10^{-5} near the TIR angle for a 10 nm gold film, while a sensitivity of 0.2% is required for the SPR regime.

This is further illustrated in Fig. 6, where we plot $\Delta R_{TM,max}$ as a function of film thickness for the TIR and SPR angles. That is, for each thickness, we obtain ΔR_{TM} vs. θ_p for the conditions of Fig. 3 in 0.1 degree increments. We then record the maximum value of ΔR_{TM} near both angles. The resulting plot clearly illustrates the transition from an SPR-dominated sensitivity for $t \geq \delta$, to a TIR-dominated response for thinner films. We have also modeled a silver film as the plasma medium (N_s=0.27+i4.18), obtaining almost identical results. In addition, for the same percentage change in index (n_a=1.000 and 1.003), our simulations with a gas as the analyte fluid show similar features, though to a much lesser degree.

4 Conclusions

We have compared 2 angular regimes for the measurement of changes in the real refractive index of bulk fluid analytes. For a fixed-angle apparatus, the method which gives the greatest change in reflectivity varies with metal film thickness. For films thicker than the skin depth,the SPR regime is the most sensitive to index changes. For thinner films, however, the TIR angle is then dominant, with increases in sensitivity on the order of 75% for 10 nm gold or silver media. Our results do not take into account specific experimental parameters such as laser linewidth, temperature and dispersion compensation, manufacturing tolerances on film thickness, etc. Including these effects may therefore modify these conclusions. Nevertheless, the potential for measuring bulk index changes in a compact, portable device with the same sensitivity as the Abbe refractometer should

prove to be an effective impetus to further research in this area.

The author appreciates useful discussions with M. Kelly and S. Kemme of Sandia National Labs, M. Descour, L. Li, and M. Mansuripur of the University of Arizona, S. Zaidi of the University of New Mexico, and J. Turner-Valle of Ball Aerospace.

Sandia is a multiprogram laboratory operated by Sandia Corp., a Lockheed Martin Company, for the United States Dept. of Energy under Contract DE-AC04-04AL85000.

References

[1] F. Jenkins and H. White, *Fundamentals of Optics, 4th Ed.*, (McGraw-Hill, New York, 1976), p. 27.

[2] D. Tentori and C. L. Famozo, "High-accuracy critical angle refractometry", *Opt. Eng.* **32**(3), 593-601 (1993).

[3] H. Raether, "Surface plasma oscillations and their applications", in *Physics of Thin Films, Vol. 9*, Edited by G. Hass, M. Francombe, and R. Hoffman (Academic Press, New York, 1977), Chap. 3.

[4] C. Nylander, B. Liedberg and T. Lind, "Gas detection by means of surface plasmon resonance", *Sensors and Actuators* **3**, 79-88 (1982/83).

[5] B. Liedberg, C. Nylander and I. Lundstrom, "Surface plasmon resonance for gas detection and biosensing", *Sensors and Actuators* **4**, 299-304 (1983).

[6] P. Daniels, J. Deacon, M. Eddowes and D. Pedley, "Surface plasmon resonance applied to immunosensing", *Sensors and Actuators* **15**, 11-18 (1988).

[7] K. Matsubara, S. Kawata and S. Minami, "Optical chemical sensor based on surface plasmon measurement", *Appl. Opt.* **27**(6), 1160-1163 (1988).

[8] L. Zhang and D. Uttamchandani, "Optical chemical sensing using surface plasmon resonance", *Electron. Lett.* **24**(23), 1469-1470 (1988).

[9] G. J. Sprokel and J. D. Swalen, "The attenuated total reflection method", in *Handbook of Optical Constants of Solids*, Edited by E. Palik (Academic Press, New York, 1991), Chap. 4.

[10] K. Welford, "Surface plasmon-polaritons and their uses", *Opt. Quant. Elec.* **23**, 1-27 (1991).

[11] N. Peyghambarian, S. Koch, and A. Mysyrowicz, *Introduction to Semiconductor Optics*, (Prentice Hall, Englewood Cliffs NJ, 1993), Sect. 3.6.

[12] M. Mansuripur, "Analysis of multilayer thin-film structures containing magneto-optic and anisotropic media at oblique incidence using 2x2 matrices", *J. Appl. Phys.* **67**(10), 6466-6475 (1990).

[13] A. E. Craig, G. A. Olson and D. Sarid, "Experimental observation of the long-range surface-plasmon polariton", *Opt. Lett.* 8(7), 380-382 (1983).

[14] D. R. Lide, *CRC Handbook of Chemistry and Physics, 77th Ed.*, (CRC Press, Boca Raton FL, 1996), p. 12-126.

FIGURE CAPTIONS

Fig. 1 - Schematic of Kretschmann-Raether configuration for exciting surface plasmons. Shown are a prism with index n_p, metal film with index N, and analyte with index n_a

Fig. 2 - Power reflectivity R_{TM} of TM-polarized field versus internal prism angle θ_p for the TIR method. The metal film thickness shown in Fig. 1 is zero. The prism index n_p=1.457 at λ=0.633 μm.

Fig. 3 - Change in reflectivity ΔR_{TM} versus θ_p for the conditions of Fig. 2.

Fig. 4 - Reflectivity R_{TM} versus θ_p for the SPR method. The metal film is gold with a complex index N_g=0.13+i3.16. The prism index is the same as in Fig. 2; the analyte index n_a=1.330.

Fig. 5 - Change in reflectivity ΔR_{TM} versus θ_p for the conditions of Fig. 4.

Fig. 6 - Maximum reflectivity change $\Delta R_{TM,max}$ as a function of film thickness for the conditions of Fig. 4. Gold film results are shown in (a), where the skin depth δ_g is approximately 32 nm; silver results are shown in (b), where δ_s is 24 nm.

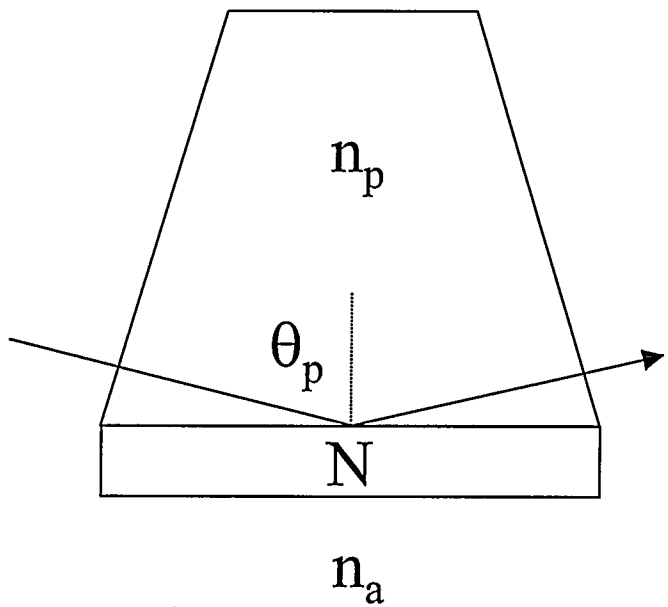
n_p
θ_p
N
n_a

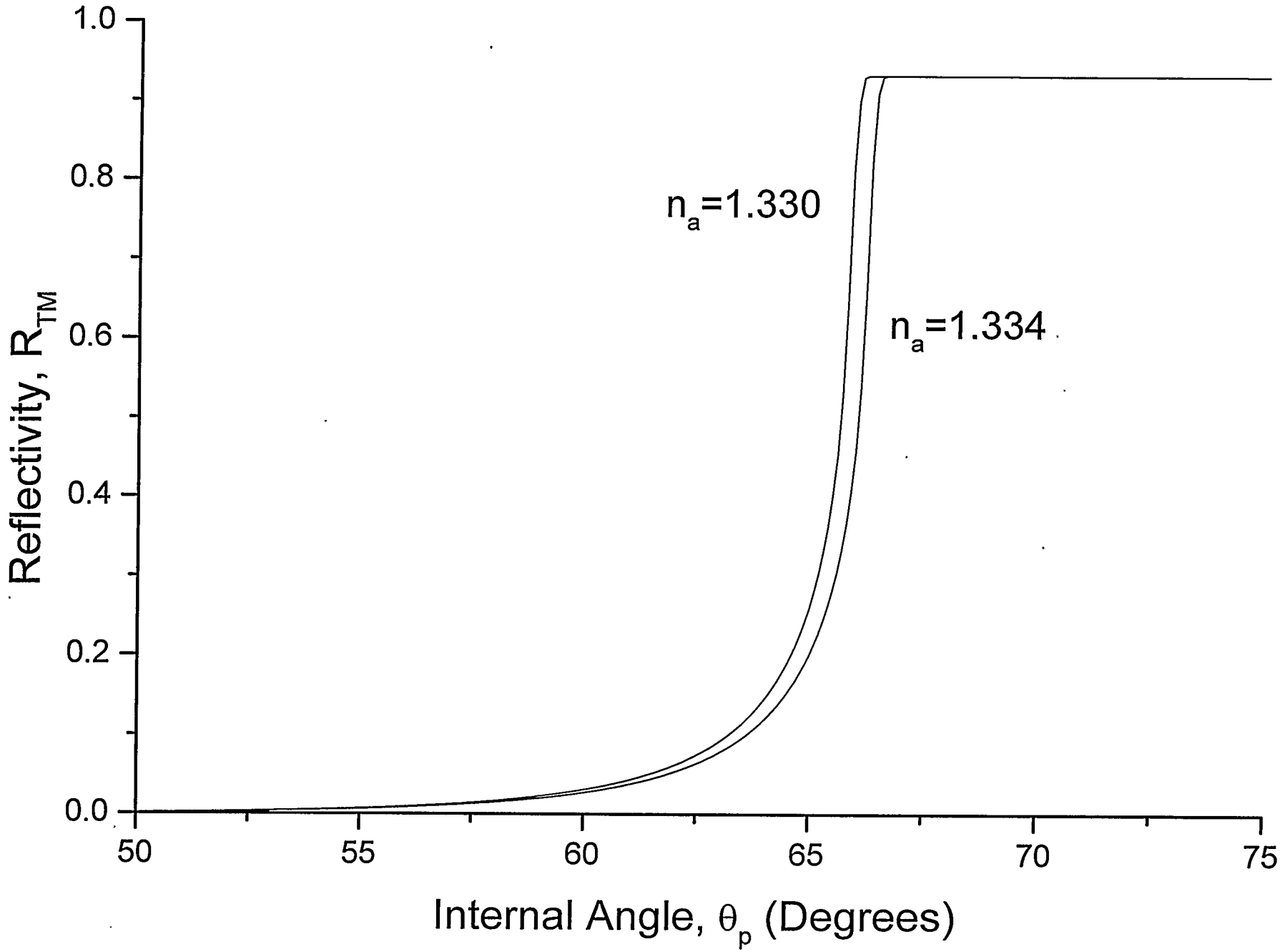
1.0
0.8
0.6
0.4
0.2
0.0
Reflectivity, R_{TM}
n_a=1.330
n_a=1.334
50
55
60
65
70
75
Internal Angle, θ_p (Degrees)

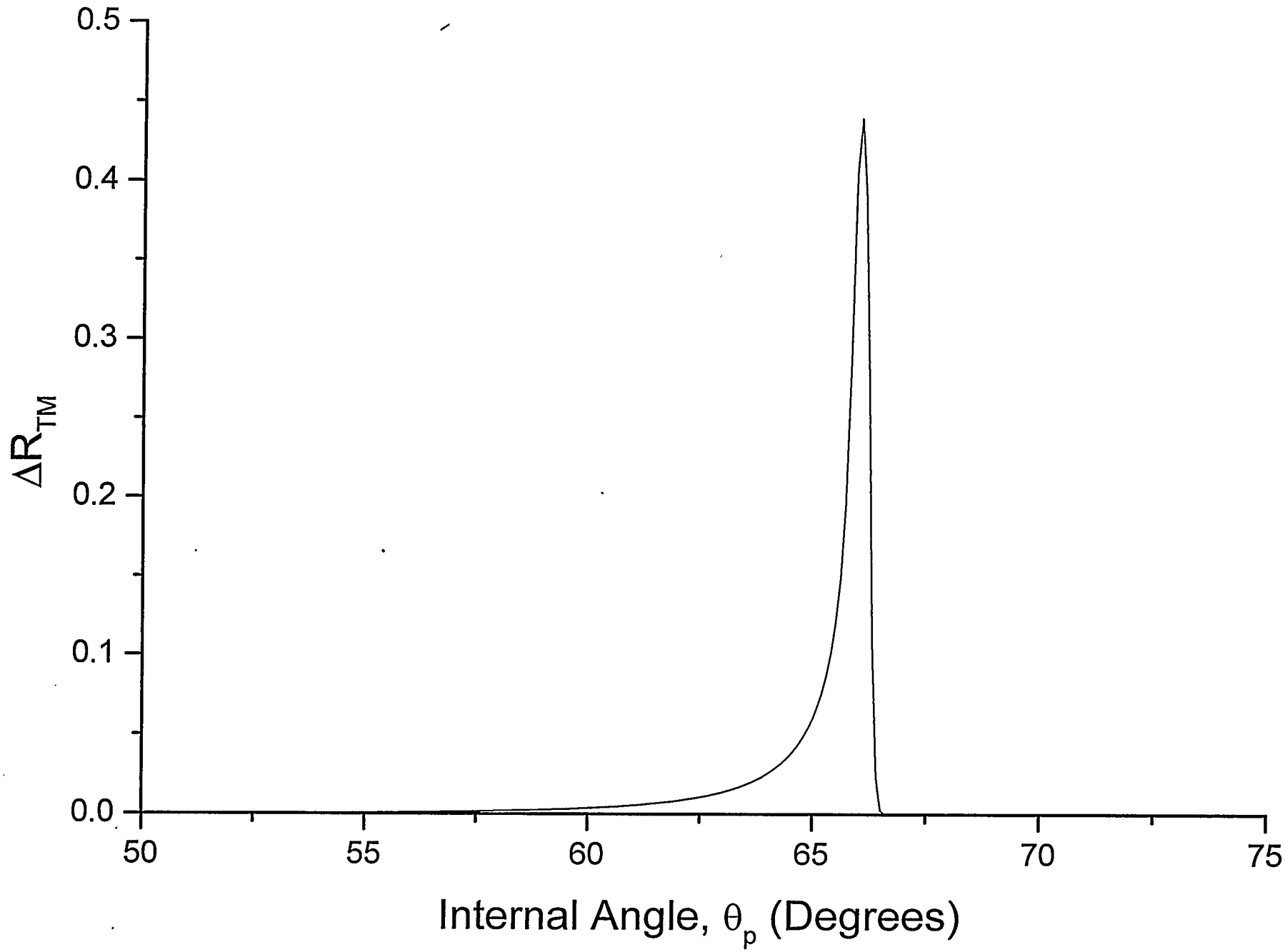
0.5
0.4
0.3
0.2
0.1
0.0
ΔR_{TM}
50
55
60
65
70
75
Internal Angle, θ_p (Degrees)

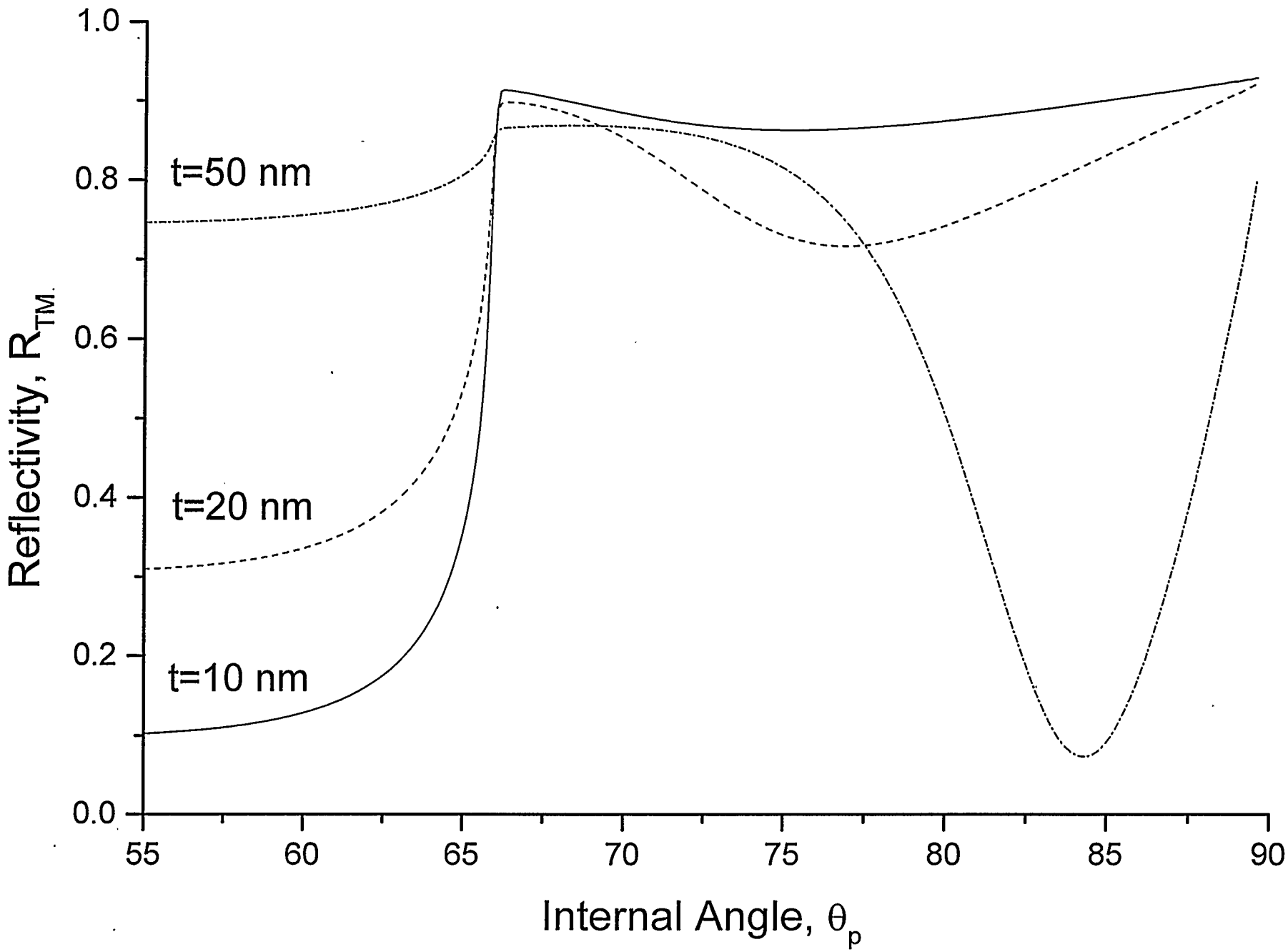
1.0
0.8
0.6
0.4
0.2
0.0
Reflectivity, R_{TM}
t=50 nm
t=20 nm
t=10 nm
55
60
65
70
75
80
85
90
Internal Angle, θ_p

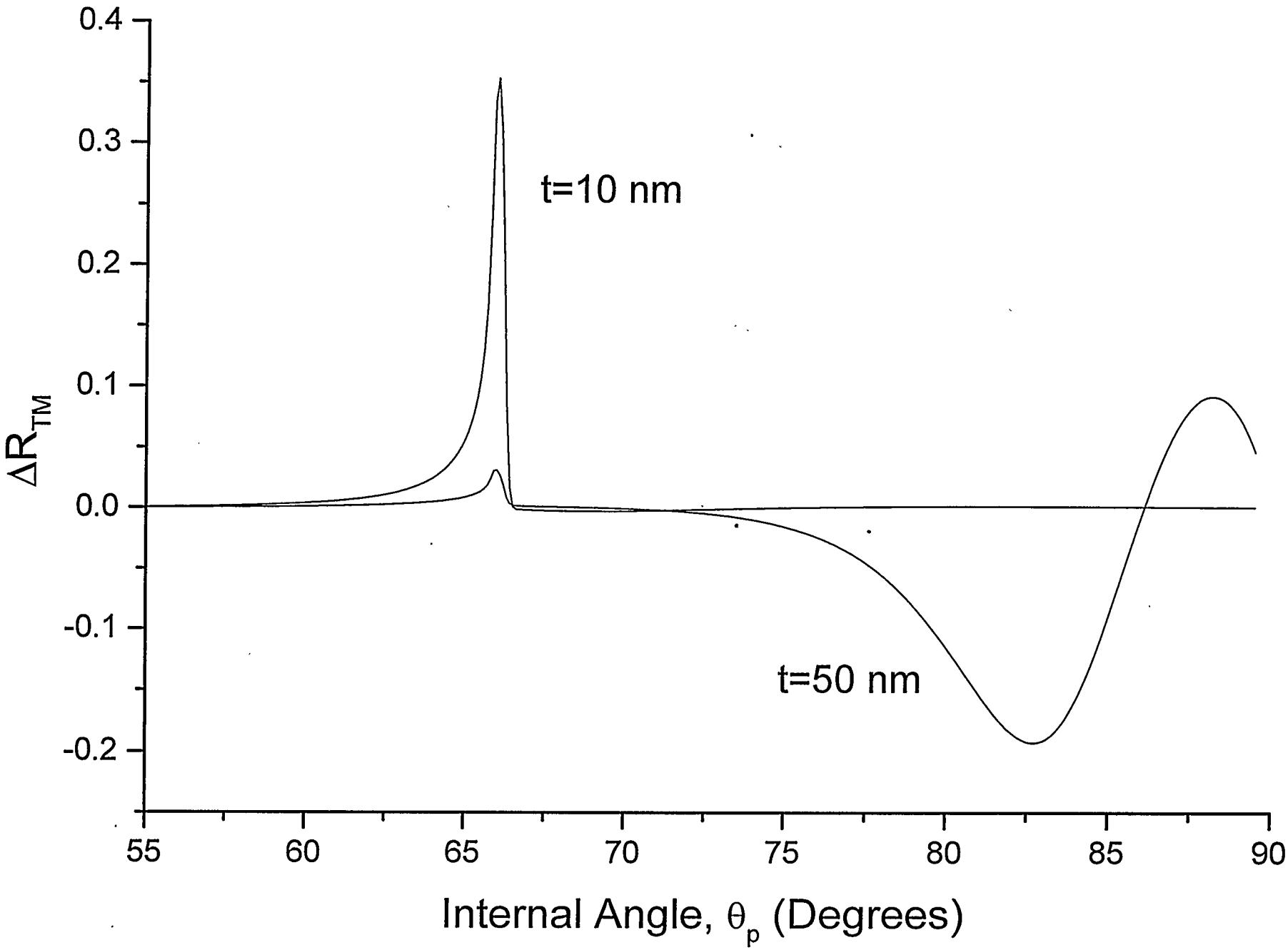
0.4
0.3
0.2
0.1
0.0
-0.1
-0.2
ΔR_{TM}
t=10 nm
t=50 nm
55
60
65
70
75
80
85
90
Internal Angle, θ_p (Degrees)

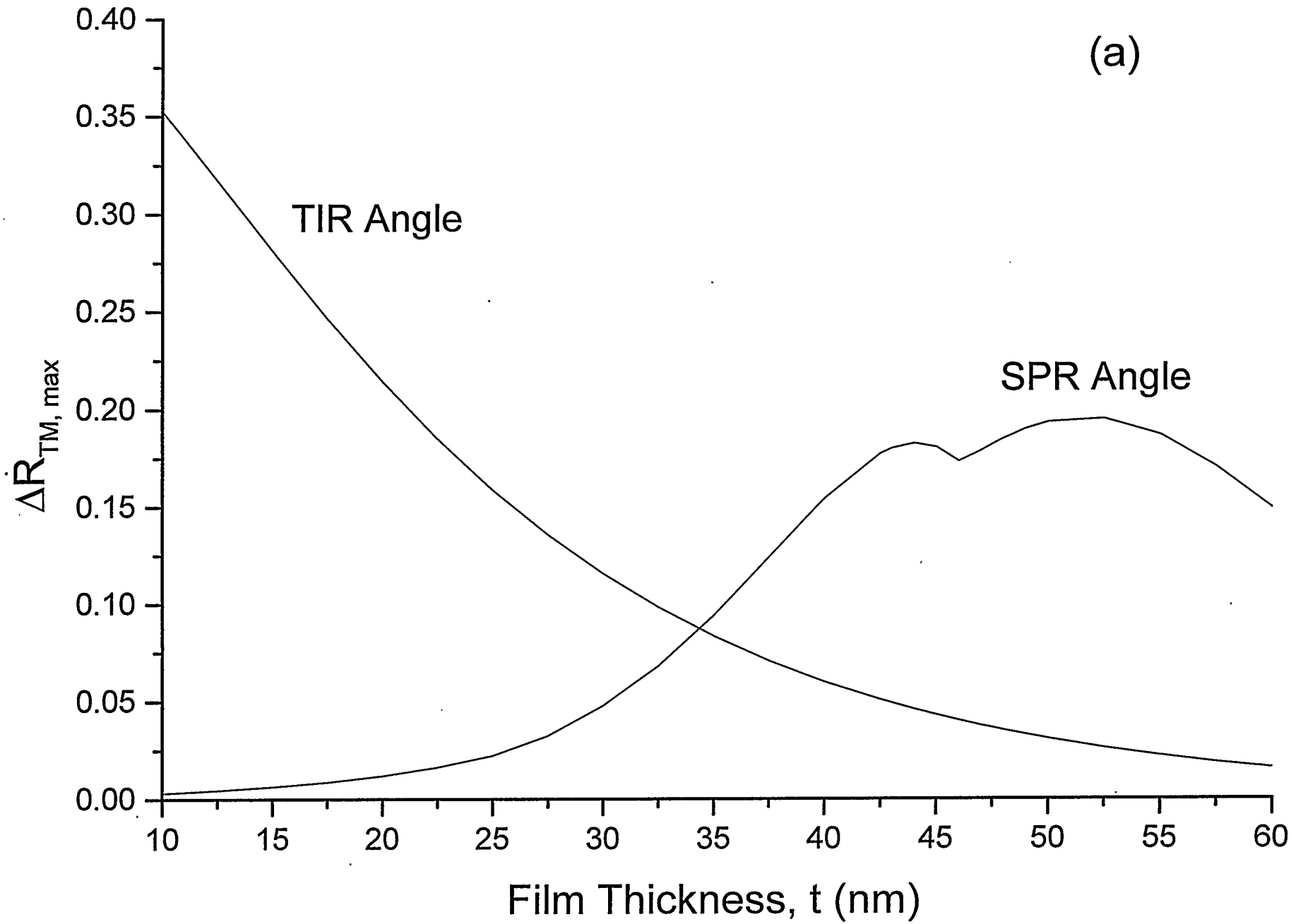
(a)
TIR Angle
SPR Angle
$\Delta R_{TM, max}$
0.40
0.35
0.30
0.25
0.20
0.15
0.10
0.05
0.00
10
15
20
25
30
35
40
45
50
55
60
Film Thickness, t (nm)

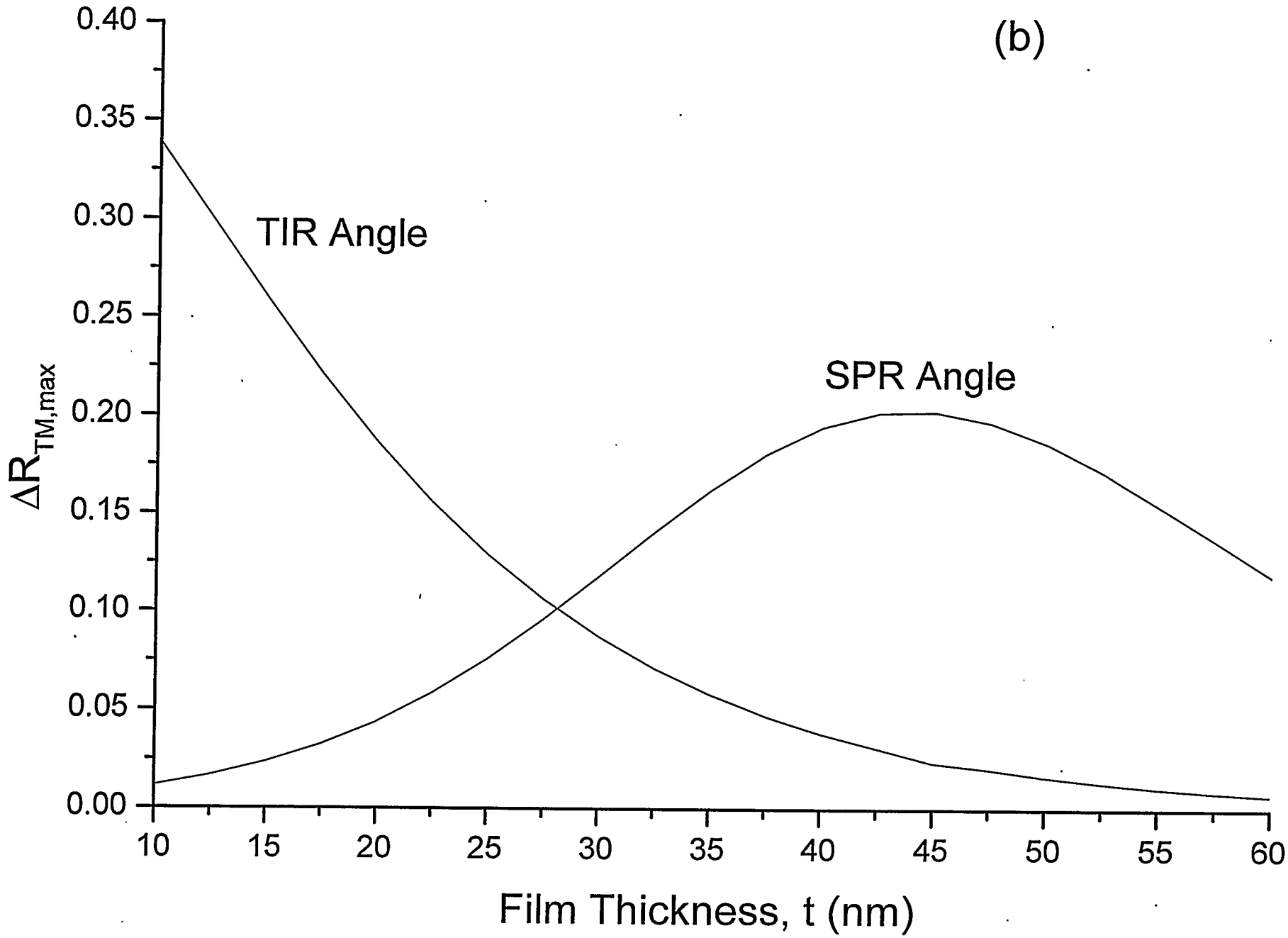
(b)
TIR Angle
SPR Angle
$\Delta R_{TM,max}$
0.40
0.35
0.30
0.25
0.20
0.15
0.10
0.05
0.00
10
15
20
25
30
35
40
45
50
55
60
Film Thickness, t (nm)